International Journal of Biochemistry and Cell Biology 112 (2019) 8–17

Contents lists available at ScienceDirect

International Journal of Biochemistry and Cell Biology

journal homepage: www.elsevier.com/locate/biocel

Comprehensive circular RNA expression profiles and the tumor-suppressive function of circHIPK3 in ovarian cancer

Fang Teng[a,1], Juan Xu[a,1], Min Zhang[b], Siyu Liu[a], Yuanyuan Gu[a], Mi Zhang[a], Xusu Wang[a], Jing Ni[c], Bing Qian[c], Rong Shen[a,*], Xuemei Jia[a,*]

[a] Department of Gynecology, Women's Hospital of Nanjing Medical University (Nanjing Maternity and Child Health Care Hospital), Nanjing 210004, China
[b] Gannan Medical University, Ganzhou 341000, China
[c] Department of Gynecologic Oncology, Jiangsu Cancer Hospital, Jiangsu Institute of Cancer Research, Nanjing Medical University Affiliated Cancer Hospital, Nanjing 210094, China

ARTICLE INFO

Keywords:
Circular RNA
Ovarian cancer
circHIPK3
Tumor-suppressive function

ABSTRACT

Background: With the development of next-generation sequencing (NGS), thousands of circular RNAs (circRNAs) have been found. Many circRNAs have been verified to play vital roles in carcinogenesis. However, whether circRNAs engage in the development and progression of ovarian cancer remains to be clarified.

Methods: We analyzed circRNA expression profiling in epithelial ovarian cancer (EOC) and normal ovarian tissues (NOT) using NGS and validated six randomly selected circRNAs via quantitative real-time-PCR (qRT-PCR), reverse-transcription PCR (RT-PCR) and Sanger sequencing after RNase treatment. CircHIPK3, the most abundant circRNA in our sequencing data, was further knocked down by siRNA. The circHIPK3 function in proliferation, invasion, migration and apoptosis of ovarian cancer cells and normal ovarian epithelial cells was analyzed via cell counting-kit 8 (CCK8), wound healing, transwell and flow cytometry analyses after circHIPK3 was efficiently silenced.

Results: Altogether, we found 7333 circRNAs, of which 4505 (61.43%) were newly identified, 2431 were significantly upregulated and 3120 were remarkably downregulated. Six randomly selected differentially expressed circRNAs were examined in 18 EOC and 18 NOT. Furthermore, the results of RT-PCR and Sanger sequencing after RNase treatment confirmed head-to-tail back-splicing. Silencing of circHIPK3 promoted proliferation, migration, and invasion and inhibited apoptosis of ovarian cancer cells (A2780 and SKOV3) and normal ovarian epithelial cells (IOSE80). Additionally, the circHIPK3-miRNA-mRNA axis was predicted as the possible mechanism using bioinformatic approaches.

Conclusions: We identified the circRNA expression profile in ovarian cancer tissues and further verified the existence and expression of six randomly selected differentially expressed circRNAs. Besides, we also found that circHIPK3 is an important regulator of ovarian cancer progression.

1. Introduction

Ovarian cancer is the most fatal malignancy in gynecologic cancer, and 60% of total patients present at advanced stages (Siegel et al., 2018). Current detection methods include contrast-enhanced computed tomography imaging and the ovarian cancer antigen CA125 measurement, but these methods are incapable of examining the cancer at early stages (Vaughan et al., 2011). The overall 5-year survival rate for patients at all stages remains at only 47% but is as low as 29% at stages III-IV (Siegel et al., 2018). Optimal cytoreductive surgery combined with platinum-based chemotherapy is the first-line treatment. However, ovarian cancer relapse and subsequent resistance to chemotherapy lead to a high mortality rate (Vaughan et al., 2011). Therefore, effective therapies are urgently needed.

Abbreviations: NGS, next-generation sequencing; circRNAs, circular RNAs; EOC, epithelial ovarian cancer; NOT, normal ovarian tissues; qRT-PCR, quantitative real-time-PCR; RT-PCR, reverse-transcription PCR; CCK8, cell counting-kit 8; ceRNA, competing endogenous RNA; CDR1as, cerebellar degeneration-related 1 antisense transcript

* Corresponding authors at: Department of Gynecology, Women's Hospital of Nanjing Medical University (Nanjing Maternity and Child Health Care Hospital), No. 123, Tianfei Xiang, Mochou Road, Nanjing 210004, China.
E-mail addresses: rongshen163@163.com (R. Shen), xmjia@njmu.edu.cn (X. Jia).
[1] These authors contributed equally to this work.

https://doi.org/10.1016/j.biocel.2019.04.011
Received 14 November 2018; Received in revised form 25 March 2019; Accepted 22 April 2019
Available online 23 April 2019
1357-2725/

It has been reported that competing endogenous RNA (ceRNA) form a complicated regulatory network in cancer development and progression (Salmena et al., 2011). As a novel class of ceRNA, circular RNAs (circRNA) are widely expressed in the mammalian transcriptome (Han et al., 2018). Currently, thousands of novel circRNAs have been identified by high-throughput sequencing and bioinformatic approaches (Jeck and Sharpless, 2014). CircRNA commonly originate from head-to-tail back-splicing of pre-mRNA in which the 5' and 3' ends are covalently linked and loop structures are formed (Barrett and Salzman, 2006). Recent studies have revealed that circulation is facilitated by reversed complementary sequences in the flanking introns as well as lariat introns and are modulated by RNA-binding proteins (Chen, 2016). Due to the lack of a 3' polyadenylated tail, most circRNA can resist the digestion of the exonuclease, whereas their linear counterpart can be degraded (Zheng et al., 2016). CircRNAs are abundant and conserved among species, but expression is specifically regulated in different tissues and developmental stages (Barrett and Salzman, 2006). Exonic circRNAs predominantly distribute in the cytoplasm and mainly act as miRNA sponges (Chen, 2016). The most well-known exonic circRNA, known as cerebellar degeneration-related 1 antisense transcript (CDR1as), harbors more than 70 binding sites of miR-7 and exerts its function primarily through sponging of miR-7 (Memczak et al., 2013).

In the current study, we investigated the expression profiles of circRNAs in epithelial ovarian cancer (EOC) and normal ovarian tissues (NOT) using RNA high-throughput sequencing. Six randomly selected circRNAs were examined in 18 EOC and 18 NOT and their expression was verified. Furthermore, we detected all six circRNAs in samples treated with RNase R and DNase, which could digest linear RNAs and genomic DNA (gDNA), respectively. The head-to-tail splicing was verified by Sanger sequencing. CircHIPK3 (hsa_circ_0000284/hsa_circRNA001123), which represents the most abundant circRNA in our data, was remarkably downregulated in EOC. Our study also found that circHIPK3 expression was significantly associated with proliferation, migration and invasion of ovarian cancer cells and normal ovarian epithelial cells. Therefore, circRNAs might play important roles in ovarian cancer progression.

2. Methods

2.1. Tissue samples and cell lines

Twenty-one NOT from patients of ages 40–71 years old with cervical cancer who underwent prophylactic oophorectomy and twenty-one high grade EOC from patients of ages between 43–77 years old were obtained from the Women's Hospital of Nanjing Medical University (Nanjing Maternity and Child Health Care Hospital) (detailed information of the ovarian cancer patients is supplied in Table S1). According to FIGO classification, 3 cases were in stage II and 18 in stage III within the 21 EOC. All of the samples were examined by hematoxylin and eosin (HE) staining and were confirmed by another pathologist. Three NOT (age: 46 ± 1.73) and three age matched EOC (age: 46.7 ± 2.31, two were classified as FIGO stage IIIc and 1 was classified as FIGO stage IIIb, and none of these three cases showed lymph nodes metastasis) were used for the subsequent next-generation sequencing. All of the patients signed informed consent forms. The protocols of this study were approved by the Ethical Committee of Women's Hospital of Nanjing Medical University (Nanjing Maternity and Child Health Care Hospital). And the methods were performed in accordance with the approved guidelines by the Ethical Committee of Women's Hospital of Nanjing Medical University (Nanjing Maternity and Child Health Care Hospital). SKOV3 were purchased from ATCC (American Type Culture Collection), and A2780 were sourced from Jiangsu KeyGEN BioTECH (KeyGEN BioTECH, Jiangsu, China). A2780 and SKOV3 were cultured in DMEM and RPMI-1640 medium (Thermo Fisher Scientific, Waltham, USA), respectively, and supplemented with 10% fetal bovine serum (Thermo Fisher Scientific, Waltham, USA), 100 U/ml penicillin and 100 μg/ml streptomycin (Thermo Fisher Scientific, Waltham, USA).

2.2. RNA sequencing

Total RNA was extracted from three EOC and three NOT using an RNeasy Mini Kit (Qiagen, Valencia, CA) according to the manufacture's instruction. The RNA purity, concentration and integrity were examined using the Bioanalyzer 2100 system (Agilent Technologies, CA, USA).

For the RNA library construction, a total of 1 μg qualified RNA per sample was used. The sequencing libraries were generated using the VAHTS Total RNA-seq (H/M/R) Library Prep Kit for Illumina® (Vazyme, NR603) following manufacturer's recommendations. Briefly, the RNA library was generated after rRNA and gDNA digestion, fragmentation, cDNA synthesis, 3'-end with A, ligation with adapters and PCR enrichment. After the quality control of the library was qualified, the clustering of the index-coded samples was performed on a cBot Cluster Generation System (Illumia, USA) according to the manufacturer's instructions. After cluster generation, the library preparations were subjected to 150 basepair (bp) paired-end sequencing using Illumina Hiseq X Ten.

The raw reads were filtered by removing the reads containing adapters and containing N of low quality, and a total of 255 million clean reads from the six samples were analyzed. The average numbers of clean reads in the NOT group and EOC group were 40.5 million (standard deviation: 0.76 million) and 44.8 million (standard deviation: 0.47 million). Hisat2 was used to align the clean reads with the H. sapiens reference genome (GRCh37/hg19, similar to the circbase reference genome). CircRNA, miRNA and mRNA were all sequenced and analyzed.

For circRNA analysis, Bowtie2 (http://bowtie-bio.sourceforge.net/bowtie2/manual.shtml) was selected to compare the clean reads with the reference genome, and the reverse shear junction was extracted from the unmapped reads using the reverse splicing (back-splice) algorithm. Finally, Bowtie2 was used to extract circRNA as a reference for follow-up analysis. For miRNA and mRNA, the aligned reads in each sample were counted using the HTseq count functionality.

Because most of the miRNAs contains the miRNA response element, it thus might function as competing endogenous RNA (ceRNA) that finally releases the inhibition of miRNA on the target gene and thus upregulates the expression of the target genes. MiRanda was used to predict the binding sites of the miRNAs as well as the miRNA targets. Finally, Cytoscape was used to visualize the network.

2.3. RNA extraction, reverse transcription (RT) and quantitative real-time PCR (qRT-PCR)

Total RNA was firstly separated by TRIzol (Invitrogen, Carlsbad, USA) and subjected to cDNA synthesis with random primers according to the instructions for the RevertAid First Strand cDNA Synthesis Kit (Thermo Fisher Scientific, Waltham, USA). For nuclear and cytoplasmic RNA separation, the PARIS Kit (Invitrogen, Carlsbad, USA) was used to partition cells into nuclear and cytoplasmic fractions. qRT-PCR was subsequently conducted using an Applied Biosystems ViiA™ 7 DX machine (Life Technologies, Carlsbad, USA) and PrimerScript RT Master Mix (Takara, Takara Island, Japan). qRT-PCR was performed under the following protocol: initial denaturation (2 min at 50 °C, 10 min at 95 °C), followed by 40 cycles at 95 °C for 15 s and 60 °C for 1 min. We analyzed the data using the $2^{-\Delta CT}$ formula and β-actin as the internal control. The primers are listed in Table S2.

2.4. Reverse-transcription PCR (RT-PCR) and Sanger sequencing

A total of 3000 ng RNA were incubated with 3 U/1000 ng RNase R (RNR07250, epicentre) for 15 min at 37 °C according to the instructions

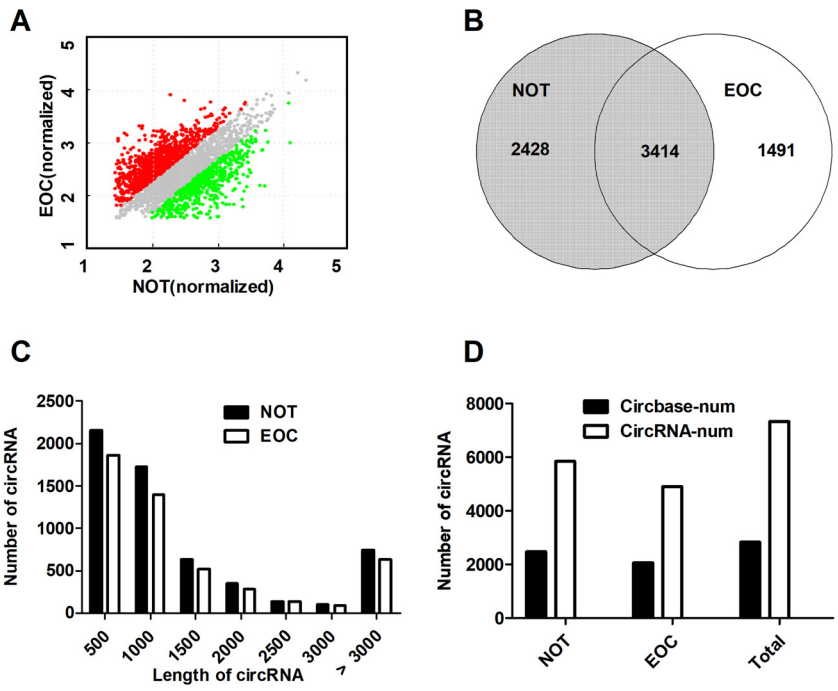

Fig. 1. Expression profiles of circRNAs in normal ovarian tissues (NOT) and epithelial ovarian cancer (EOC). A: Scatter-plot of the differentially expressed circRNA between NOT and EOC. The values on the x- and y-axes correspond to the normalized signal values of the two types of tissues **(log2** scale). The red dots represent upregulated circRNAs, and the green dots indicate downregulated circRNAs with fold change > 2 and $p < 0.05$. B: Number of circRNA identified in NOT and EOC by RNA sequencing. Only 3414 circRNAs were observed in both groups. C: Length distribution of circRNAs identified in NOT and EOC. Most circRNAs were less than 1500 bp. D: Number of circRNA detected in circbase and our sequencing result. Almost half of the total circRNAs were newly identified circRNA in our sequencing data.

of the RNAse R. The RNA was purified using the RNeasy MinElute Cleanup Kit. Subsequently, DNase was used to remove genomic DNA according to the manufacture's protocol. The control group was treated with nuclease-free water.

Then the RNase R and DNase treated RNA and control RNA were subjected to cDNA synthesis with random primers according to the instructions for the RevertAid First Strand cDNA Synthesis Kit (Thermo Fisher Scientific, Waltham, USA). Subsequently, PCR was performed and the PCR products of the circRNA were analyzed by Sanger sequencing using the primers listed in Table S2.

2.5. siRNA transfection

SiRNA were synthesized by Ribobio (Guangzhou, China) according to the sequence described by Zheng et al (Zheng et al., 2016). The siRNA targeting the back-splicing junction of circHIPK3 was 5'-CUAC AGGUAUGGCCUCACA-3'. The siRNA was transfected using Lipofectamine 2000 transfection reagent (Thermo Fisher Scientific, Waltham, USA) according to the manufacturer's instructions. All of the experiments were conducted in triplicate and repeated at least three times.

2.6. Wound healing assay

The wound healing assay was performed according to the protocol described before (Memczak et al., 2013). A2780 and SKOV3 cells were seeded in a six-well plate and scratched using 200 μL pipette tips after reaching 95–100% confluency, and after injury, the cells were cultured in serum-free DMEM or RPMI-1640 medium respectively. The cells were photographed at 0 h and 24 h after injury under an EVOS XL Core digital microscope (Thermo Fisher Scientific, Waltham, USA).

2.7. Transwell assay

The migration and invasion assays were conducted using the transwell (Corning, NY, USA) assay with and without Matrigel (BD Science, Bedford, USA), respectively, according to the protocol described before (Xu et al., 2013). Approximately 3–5 × 10^4 cells were seeded in the upper chambers with 200 μL serum-free medium. Medium containing 20% FBS was added to the lower chambers. After 24–72 h incubation, cells were fixed with 4% paraformaldehyde and stained with 1% crystal violet. Cells in the upper chambers were scraped, and cells in the lower chambers were lysed by RIPA lysis buffer (Invitrogen, Carlsbad, USA). The absorbance was examined using a microplate reader (BioTek Synergy H4) at a wavelength of 562 nm (BioTek Instruments, Vermont, USA).

2.8. Cell counting kit-8 assay

The proliferation of A2780 and SKOV3 cells was analyzed using the cell counting kit-8 (CCK-8) (KeyGEN BioTECH, Jiangsu, China) according to the manufacture's protocol. After 24 h transfection, approximately 1 × 10^3 cells were seeded in each well of 96-well plates. The optical density was detected at 0 h, 24 h, 48 h and 72 h after transfection by a BioTek Synergy H4 instrument at 450 nm (BioTek Instruments, Vermont, USA).

2.9. Apoptotic cell detection

Cells were stained with PE and Annexin V using the PE-Annexin V Apoptosis Detection kit (BD Biosciences, San Diego, USA) at 48 h after transfection according to the manufacture's protocol. Cell apoptosis was analyzed under a flow cytometer (Beckman, CA, USA). For IOSE80 cells, the apoptosis was analyzed after inducing by the apoptosis inducer according to the Apoptosis Anducers Kit's instruction (Beyotime, Shanghai, China).

2.10. Statistical analysis

Statistical analysis was conducted using GraphPad Prism 5. Data are presented as mean ± SEM. The data were analyzed using Student's *t*-test, for which $p < 0.05$ was considered statistically significant.

2.11. Data availability statement

All data generated or analyzed during this study are included in this published article (and the Supplementary files).

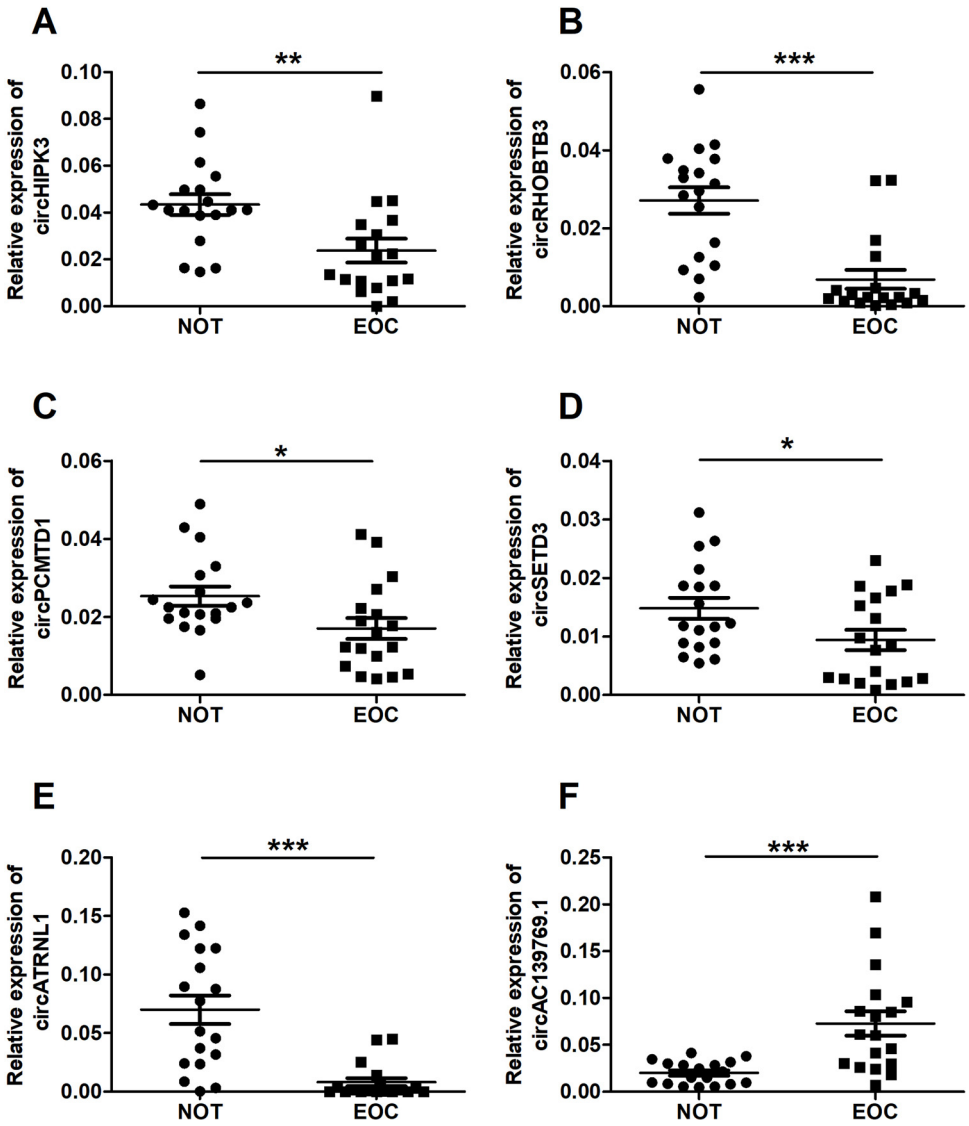

Fig. 2. Validation of circRNAs expression in NOT and EOC by qRT-PCR with divergent primers. The relative expression levels of the 5 downregulated circRNAs (A–E) and 1 upregulated circRNA (F) in 18 NOT and 18 EOC were determined by qRT-PCR with divergent primers. β-actin was used as the internal control. The results are presented as the mean ± SEM. $^{*}p < 0.05$, $^{**}p < 0.01$, $^{***}p < 0.001$.

3. Results

3.1. Expression profiles of circRNAs in NOT and EOC

To investigate circRNAs function in NOT and EOC, we firstly examined the dysregulated circRNAs via RNA sequencing. Three NOT from cervical cancer patients underwent prophylactic oophorectomy, and three EOC were sequenced and analyzed. In total, 7333 circRNAs were identified, of which 2431 circRNAs were upregulated (red spots), and 3120 circRNAs were downregulated (green spots) with fold-changes ≥ 2 and p-value < 0.05 (Fig. 1A, Table S3). We found that a variety of circRNAs were expressed uniquely among tissues. In the current study, 2428 circRNAs were specific to NOT, 1491 circRNAs were only expressed in EOC, and only 3414 circRNAs were observed in both groups (Fig. 1B). We also explored the length distribution of circRNA and found that most circRNAs were shorter than 1500 bp (Fig. 1C), consistent with previous studies (Zheng et al., 2016). Moreover, of all 7333 circRNA disclosed in this study, only 2828 (38.57%) were overlapped with circBase (http://www.circbase.org/) and 4505 (61.43%) were newly identified (Fig. 1D, Table S4).

3.2. Validation of deregulated circRNAs

To verify the differentially expressed circRNAs in our sequencing results, we randomly selected six circRNAs according to the following criteria: (1) highly abundant circRNAs and (2) fold-change > 2 and p-value < 0.01. CircRNAs expression was validated in 18 NOT and 18 EOC by qRT-PCR with divergent primers. As shown in Fig. 2, the levels of circHIPK3 (hsa_circ_0000284), circRHOBTB3 (hsa_circ_0007444), circPCMTD1 (hsa_circ_0001801), circSETD3 (hsa_circ_0000567) and circATRNL1 (hsa_circ_0020093) were significantly decreased, whereas that of circAC139769.1, a newly found circRNA, was dramatically increased in the EOC group compared with those in the NOT group ($^{*}p < 0.05$, $^{**}p < 0.01$, $^{***}p < 0.001$).

To exclude head-to-tail splicing from trans-splicing or genomic rearrangements, we validated the six candidate circRNAs by analyzing their expression before and after RNase R and DNase treatment by PCR and examined their splicing by Sanger sequencing (Fig. 3A–F). In one group, RNA extracted from A2780 cells was first digested with RNase, followed by treatment with DNase, and RNA was treated only with water in the control group. The expression of circRNA(c) and linear mRNA (m) or lncRNA (long noncoding RNA, lnc) was detected in the

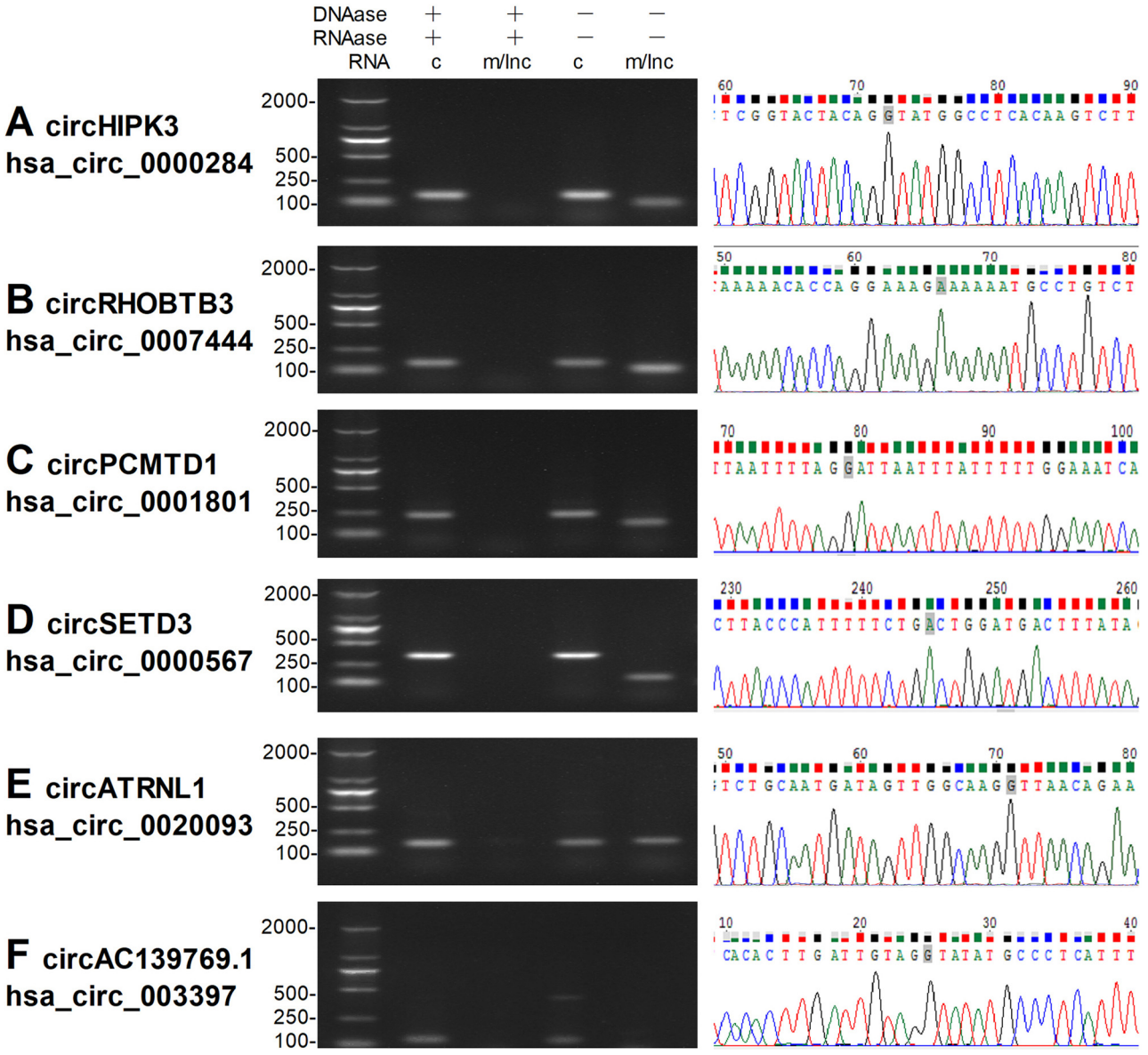

Fig. 3. Circular RNA validation. A-E: (Left) Reverse-transcription PCR (RT-PCR) was conducted to detect the expression of circRNA (c) and mRNA (m) in RNA treated with or without RNase R and DNase in A2780 cells. (Right) Sanger sequencing result of the RT-PCR products on the left. The base colored in gray indicates the head-to-tail splicing sites. F: (Left) The expression of circAC139769.1 and its linear isoform lncAC139769.1 was investigated by RT-PCR. (Right) Sanger sequencing result of circAC139769.1 RT-PCR products. The base colored in gray indicates the head-to-tail splicing sites.

two groups. As shown in Fig. 3A–D, only circRNA can be observed in the RNase R and DNase treated samples (Fig. 3, Lane 1 and 2), whereas both linear and circular RNA can be detected in the control group (Fig. 3, Lane 3 and 4). This result indicated that RNase could eliminate linear mRNA while preserving circRNA. Interestingly, the ATRNL1 mRNA is partially resistant to RNase digestion and is present at a notably low level after RNase digestion (Fig. 3E, Lane 2). We also observed that rolling cycle cDNA products occur in the control group, which could also be eliminated by RNase (Fig. 3F). We failed to detect the expression of linear RNA of AC139769.1 as a result of its high similarity to another gene known as RPSAP58. Moreover, the PCR products were confirmed by Sanger sequencing. The base colored in gray shows the head-to-tail splicing sites (Fig. 3).

3.3. Expression of circHIPK3 in ovarian cancer cells

Among the six circRNAs that were validated above, circHIPK3 was the most abundant circRNA in our sequencing data and attracted our attention (Fig. 2A). Therefore, we further investigated the function of circHIPK3 in ovarian cancer cells. First, circHIPK3 expression in ovarian cancer cell lines (HO8910, A2780, OVCAR8, COC1 and SKOV3) and the immortalized normal ovarian epithelial cell line (IOSE80) was examined by qRT-PCR. Consistent with the expression profile of circHIPK3 in EOC and NOT, circHIPK3 was highly expressed in normal ovarian tissue cells (IOSE80 cells) compared with that in ovarian cancer cell lines (Fig. 4A). In the ovarian cancer cell lines, circHIPK3 expression was higher in A2780 and SKOV3 cells than in other cells and thus was chosen for silencing of circHIPK3 during the subsequent experiments (Fig. 4A). Commonly, the function of circRNAs is closely related to their location in cells (Han et al., 2018). We investigated the distribution of circHIPK3 in ovarian cancer cells. Using 12S and 45S RNA as the cytoplasmic and nucleus RNA control, respectively, we found that circHIPK3 was primarily distributed in the cytoplasm (Fig. 4B). Additionally, we found that only circHIPK3 was significantly downregulated after si-circHIPK3 transfection, by 44.9% in A2780, 55.9% in SKOV3 and 55.6% in IOSE80 (Fig. 4C, Fig. S2A), whereas the linear

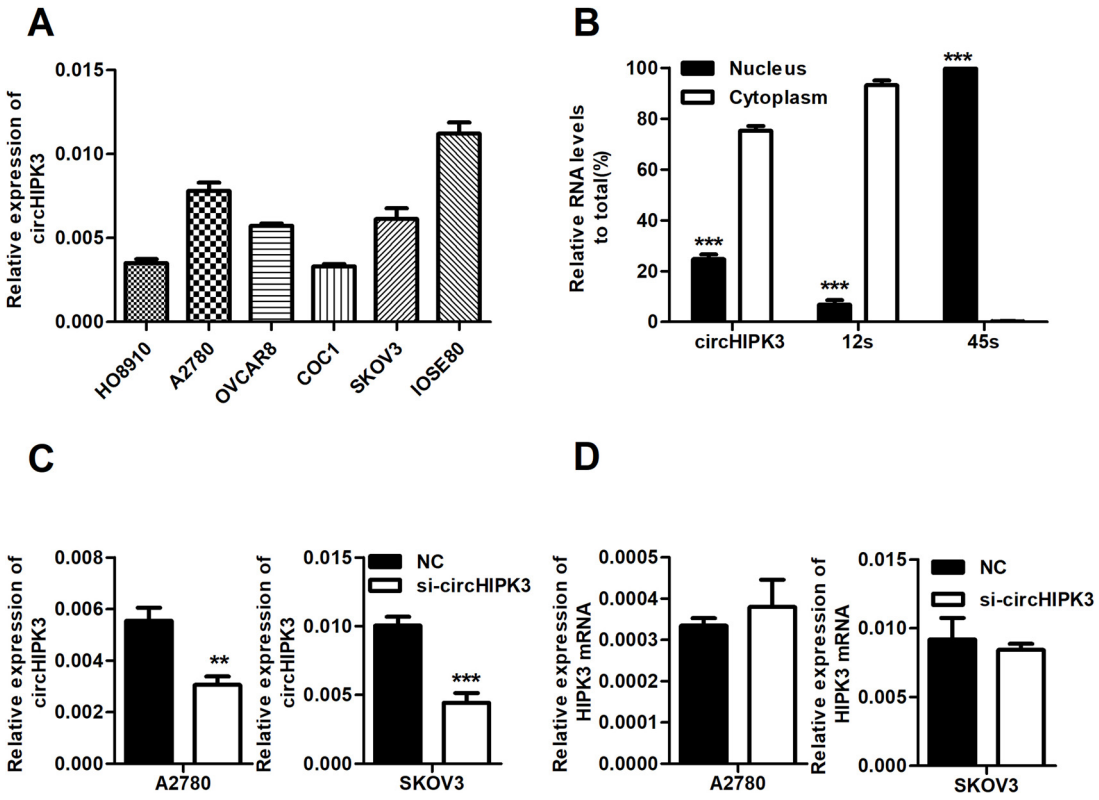

Fig. 4. Expression of circHIPK3 in ovarian cancer cells and knockdown efficiency of circHIPK3 siRNA. A: qRT-PCR detection of the expression levels of circHIPK3 among 5 ovarian cancer cell lines (HO8910, A2780, OVCAR8, COC1 and SKOV3) and 1 normal ovarian epithelium cell line (IOSE80). B: RNA isolated from the cytoplasm and nucleus of A2780 ovarian cancer cells were analyzed by qRT-PCR. CircHIPK3 were mainly distributed in the cytoplasm, similar to the 12S control. C and D: Si-circHIPK3 only knocked down the circHIPK3 (C) but not their linear HIPK3 mRNA (D) in A2780 and SKOV3 cells. Data are shown as the mean ± SEM. $^{***}p < 0.001$.

HIPK3 mRNA counterparts were not significantly changed in both A2780 and SKOV3 cells (Fig. 4D).

3.4. Silencing of circHIPK3 significantly promoted the invasion and migration of ovarian cancer cells and normal ovarian epithelial cells

After circHIPK3 was successfully knocked down in ovarian cancer cells, we further examined the invasion and metastasis of ovarian cancer cells. As shown in Fig. 5A and B, silencing of circHIPK3 could significantly promote the migration of ovarian cancer cells compared with that in the negative control group. Consistent with the wound-healing results, downregulation of circHIPK3 significantly promoted migration and invasion of A2780 and SKOV3 cells, as shown in the transwell assay ($^{*}p < 0.05$, Fig. 5C and E). The results indicate that knockdown of circHIPK3 markedly enhanced migration and invasion of A2780 and SKOV3 cells ($^{*}p < 0.05$, Fig. 5D and F). Besides, we also examined the effects of circHIPK3 knock-down on the migration and invasion ability of IOSE80 cells. The results indicated that knock-down of circHIPK3 could also promote migration and invasion of IOSE80 cells ($^{**}p < 0.01$, $^{***}p < 0.001$, Fig. S2C and S2D).

3.5. Downregulation of circHIPK3 increased cell proliferation and decreased cell apoptosis of ovarian cancer cells and normal ovarian epithelial cells

As an important indicator of the malignant behavior of cancer cells, cell proliferation and apoptosis was further examined. As shown in Fig. 6A and B and Figure S2B, cell proliferation was markedly increased in the circHIPK3 knockdown ovarian cancer cells and normal ovarian epithelial cells at 48 h and 72 h after seeding ($^{*}p < 0.05$, $^{**}p < 0.01$, $^{***}p < 0.001$). Flow cytometry analysis indicated that cell apoptosis was significantly decreased in the circHIPK3 knockdown ovarian cancer cells and normal ovarian epithelial cells (Fig. 6C–D and Figure S2E-F, $^{**}p < 0.01$, $^{***}p < 0.001$).

3.6. Possible mechanism of circHIPK3 in ovarian cancer progression

According to previously reported results (Zheng et al., 2016; Shan et al., 2017; Li et al., 2017; Zeng et al., 2018), circHIPK3 (hsa_circ_0000284) primarily functions through the circHIPK3-miRNA-mRNA axis. Therefore, ceRNA analysis of circHIPK3 was also performed. Our results also supported the observation that circHIPK3 might play an important role in EOC through the circHIPK3-miRNA-mRNA axis (Fig. 6E). We collected 12 miRNAs that have 1–3 binding sites in circHIPK3, as reported previously (Zheng et al., 2016), or that were expressed with high abundancy in our sequencing results, and we also predicted their possible target genes via miRanda (Table S5-6). Cytoscape was performed to visualize the network (Fig. 6E).

4. Discussion

With the development of NGS, thousands of circRNAs have been found. Many circRNAs have been verified to play vital roles in carcinogenesis, including cell proliferation, apoptosis, migration and invasion (Wang et al., 2017; Zhong et al., 2017; Chen et al., 2017). One study analyzed circRNAs expression in primary ovarian cancer tissues and their lymph nodes and in peritoneum metastatic cancer tissues (Ahmed et al., 2016). In the current study, we further explored the differently expressed circRNAs in EOC and NOT using high throughput sequencing. Compared with NOT, 2431 and 3120 circRNAs were distinctly upregulated and downregulated in EOC, respectively.

To further explore circRNAs that might exert an important function

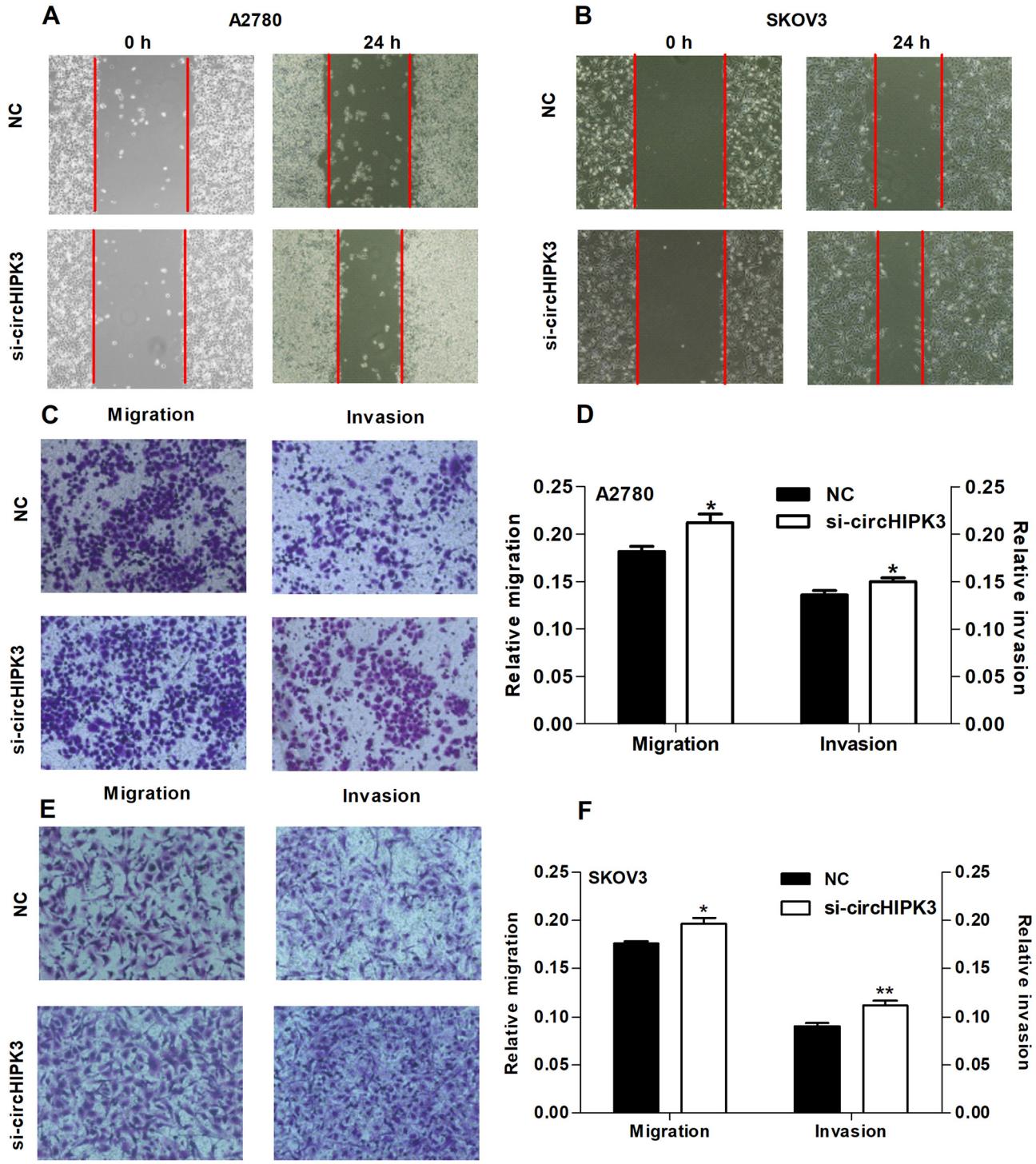

Fig. 5. Silencing of circHIPK3 promoted migration and invasion of ovarian cancer cell lines. A and B: The migration potential of cells transfected with the circHIPK3 siRNA and control was determined by the wound healing assay at 24 h after injury in A2780 and SKOV3 cells. C: Cell migration and invasion capabilities of A2780 cells were evaluated by transwell assay without (migration) and with (invasion) Matrigel assays. D: The protein concentration of the migrated and invaded A2780 cells was analyzed using a microplate reader at a wavelength of 562 nm. E and F: The cell migration and invasion potential of cells transfected with circHIPK3 siRNA and control were repeated in SKOV3 cells in the transwell assay. The results are shown as the mean ± SEM. $^{*}p < 0.05$, $^{**}p < 0.01$.

in EOC, we validated six circRNAs that were significantly differentially expressed, and the qRT-PCR results are consistent with the sequencing data, which indicated that the sequencing data are credible.

Previous studies revealed that circRNAs can resist RNase digestion, while mRNAs are not (Memczak et al., 2013). Other studies indicated that linear RNA with no 3' overhang or with only a 4-nucleotide overhang could resist RNase digestion (Barrett and Salzman, 2006). As shown in Fig. 3, RNase could digest linear mRNA while preserving circRNA. However, ATRNL1 mRNA which has no overhang was not eliminated completely. In addition, a ladder could appear on the agarose gel as a result of the rolling cycle cDNA products (You et al., 2015). We also found that circAC139769.1 rolling cycle cDNA products appeared in A2780 cells (Fig. 3F), and this phenomenon could also verify the circular structure indirectly. Besides, circAC139769.1 is

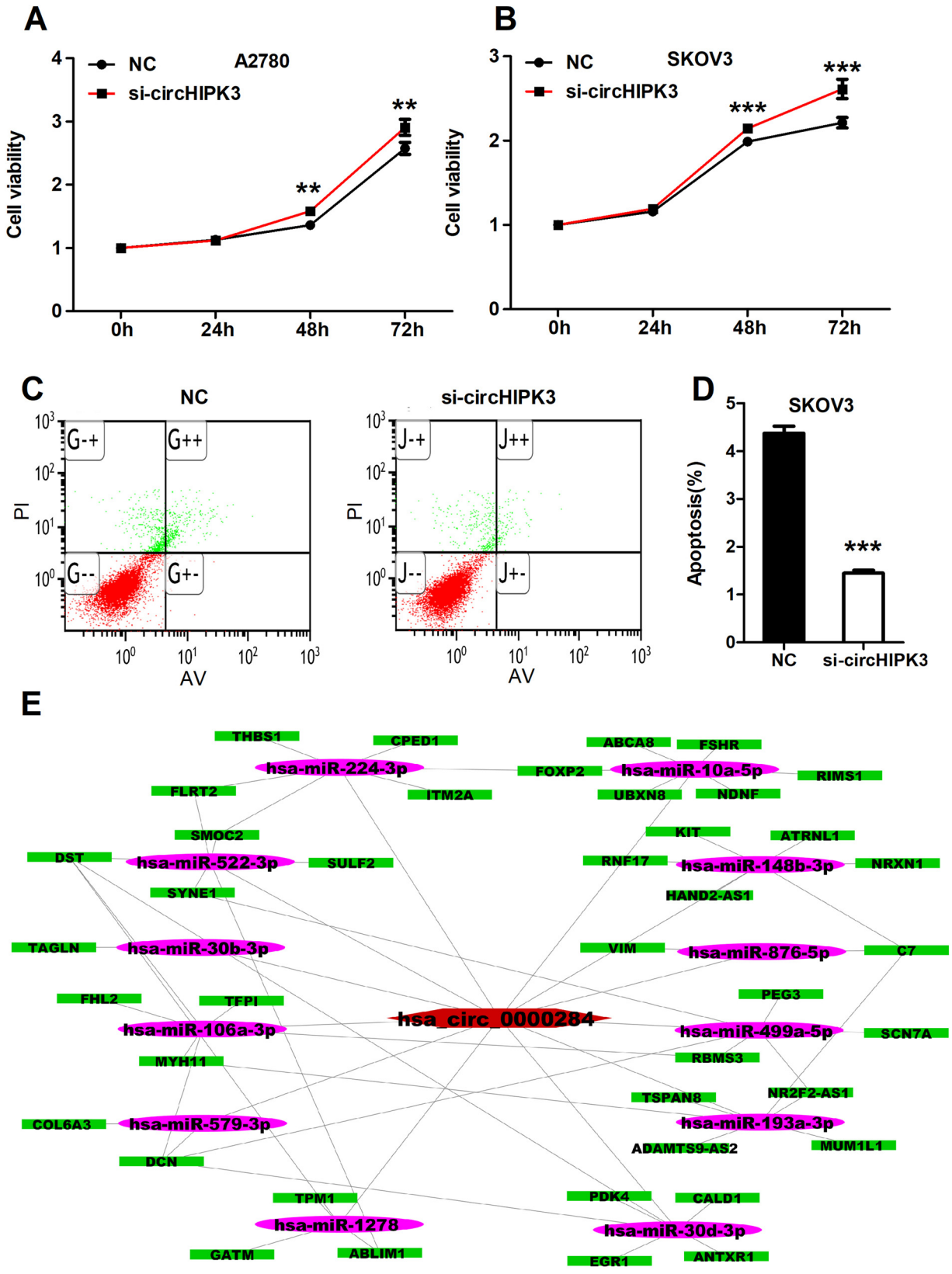

Fig. 6. Knockdown of circHIPK3 promoted cell proliferation and attenuated cell apoptosis. A and B: Cell proliferation of A2780 and SKOV3 cells treated with circHIPK3 siRNA was examined by cell counting Kit-8 (CCK-8) assay at the indicated timepoint. C: At 48 h following transfection, SKOV3 cells were stained by PE and Annexin V, and the stained cells were analyzed by flow cytometry. D: The apoptosis cell percentage (percentage of both the upper and lower right quadrant cells) was compared between the two groups. Data are presented as the mean ± SEM. $^{***}p < 0.001$, $^{**}p < 0.01$. E: CeRNA analysis for circHIPK3 (hsa_circ_0000284). Based on the circRNA, miRNA and mRNA sequencing data, MiRanda and Cytoscape were performed to reveal the network of circHIPK3-miRNA-mRNA. Twelve candidate miRNA and their possible target genes were involved. CircHIPK3 is located in the center, pink ellipses represent miRNA and green rectangles represent mRNA. The association among the nodes is indicated by solid lines.

formed by the longest exon of LncAC139769.1 (1718 bp), the other exons of LncAC139769.1 are quite short (213 bp in total) and are overlapped with part of the RPSAP58 gene. Therefore, we didn't find the specific primer for the linear RNA. However, further studies about the circAC139769.1 are needed in the future.

To confirm the possible function of circRNAs in EOC, we selected circHIPK3, which is the most abundant circRNA in our data, to explore its effects on ovarian cancer cells. Consistent with the previous study (Zheng et al., 2016), circHIPK3 was expressed principally in the cytoplasm of A2780 ovarian cancer cells. The previous studies indicated that silencing of circHIPK3 could attenuate retinal endothelial cell and HEK-293 T cell proliferation (Zheng et al., 2016; Shan et al., 2017), whereas over-expression of circHIPK3 decreased invasion and migration of bladder cancer cells (Li et al., 2017). In contrast, circHIPK3 knockdown inhibited colorectal cancer cell migration and invasion and promoted apoptosis (Zeng et al., 2018). These results indicate that circRNA might exhibit different effects in different cells or tissues. In our study, circHIPK3 was decreased in the EOC group (Fig. 2A), and knockdown of circHIPK3 increased cell proliferation, promoted migration and invasion, and inhibited apoptosis of both the normal ovarian epithelial cells (IOSE80) and ovarian cancer cells (A2780 and SKOV3) in our study (Fig. 5, Fig. 6A–C, Fig. S2B-F), which might be attributed to cell-type-specific expression and function.

The mechanism involved in circRNA regulation had not been clarified. An increasing number of investigations have indicated that circRNAs might function as miRNA sponges to modulate the function of miRNA targets (Hansen et al., 2013; Wang et al., 2016). CircHIPK3 was observed to sponge miR-558 in bladder cancer cells (Li et al., 2017), miR-30a-3p in diabetes mellitus (Shan et al., 2017), miR-7 in colorectal cancer (Zeng et al., 2018) and miR-124 in HeLa cells (Zheng et al., 2016). Unlike CDR1as, which contain more than 70 binding sites of miR-7 (Hansen et al., 2013), circHIPK3 was reported to contain 18 binding sites of 9 miRNAs (Zheng et al., 2016). In our study, we found that circHIPK3 possessed only 1–3 binding sites of each miRNA. Twelve miRNAs, i.e., miR-10a-5p, miR-224-3p, miR-876-5p, miR-148b-3p, miR-30d-3p, miR-193a-3p, miR-579-3p, miR-499a-5p, miR-106a-3p, miR-1278, miR-30b-3p and miR-522-3p, were predicted as the possible target of circHIPK3 in ovarian cancer, suggesting that circHIPK3 might exert an important function by sponging miRNAs (Fig. 6E). Among which, miR-10a-5p, is the most abundant miRNAs related to circHIPK3. And several studies have shown that miR-10a can promote the progression of a variety of cancers, such as the cervical cancer (Long et al., 2012), acute myeloid leukaemia (Bryant et al., 2012), pancreatic cancer (Weiss et al., 2009). Additionally, a miR-106a inhibitor was observed to suppress the growth of ovarian cancer in xenograft mice (Cai et al., 2016). MiR-148b was upregulated in 92.21% (71/77) of ovarian cancer tissues and might play an important role in the early stage of ovarian cancer (Chang et al., 2012). Thus, circHIPK3 might exert its function in ovarian cancer by sponging one or several of the miRNAs. However, further studies are still needed to confirm which miRNAs are sponged by circHIPK3.

Several studies also have revealed that circRNAs might exert a regulatory function via interaction with proteins (Du WW et al., 2017a). Circ-Amotl1 was observed to facilitate c-myc translocation from cytoplasm to the nucleus, resulting in tumorigenesis of breast cancer (Yang et al., 2017). CircFoxo3 induces cardiac senescence by retaining anti-senescence proteins in the cytoplasm (Du WW et al., 2017b). Herein, we speculated that circHIPK3 might also exert its regulatory effects through interaction with proteins. Further analysis should be conducted to confirm the possible mechanism involved in circHIPK3 regulation.

5. Conclusions

In conclusion, we analyzed circRNA expression profiling in EOC and NOT using RNA high-throughput sequencing. Six circRNAs were further validated in EOC and NOT by qRT-PCR and subsequently confirmed to resist to RNase digestion. Of these circRNAs, circHIPK3 siRNA could promote proliferation, migration and invasion and inhibit apoptosis of SKOV3 and A2780 ovarian cancer cells as well as IOSE80 cells. The possible mechanism was also predicted using a bioinformatics method. Our investigation indicates that circHIPK3 is an important regulator of ovarian cancer progression.

Funding

This work was supported by the National Natural Science Foundation of China (grant number: No. 81572556, No. 81602285 and No. 81872126), Nanjing Medical Science and technique Development Foundation (No. ZKX15046, No. ZDX16015, QRX17159 & No. JQX17009) and Jiangsu Provincial Medical Talent (Xuemei Jia).

Authors' contributions

TF and XJ performed the experimental work and drafted the manuscript. SR and JXM supervised and designed the research. ZM, GYY, LSY, WXS, NJ, QB participated in the experiments, discussion and interpretation of data. SR, ZM, GYY, LSY, WXS, NJ, QB revised the manuscript. All authors have read and approved the final manuscript.

Competing interests

The authors report no competing interests.

Appendix A. Supplementary data

Supplementary material related to this article can be found, in the online version, at doi:https://doi.org/10.1016/j.biocel.2019.04.011.

References

Ahmed, I., Karedath, T., Andrews, S.S., Al-Azwani, I.K., Mohamoud, Y.A., Querleu, D., et al., 2016. Altered expression pattern of circular RNAs in primary and metastatic sites of epithelial ovarian carcinoma. Oncotarget 7, 36366–36381. https://doi.org/10.18632/oncotarget.8917.

Barrett, S.P., Salzman, J., 2006. Substrate recognition and catalysis by the exoribonuclease RNase r. J. Biol. Chem. 281 (40), 29769–29775. https://doi.org/10.1074/jbc.M606744200.

Bryant, A., Palma, C.A., Jayaswal, V., Yang, Y.W., Lutherborrow, M., Ma, D.D., 2012. miR-10a is aberrantly overexpressed in Nucleophosmin1 mutated acute myeloid leukaemia and its suppression induces cell death. Mol. Cancer 11, 8. https://doi.org/10.1016/j.surg.2011.06.017.

Cai, Z.H., Chen, L.M., Liang, Y.J., Shi, J.R., You-Ju, M.A., Wang, W.M., et al., 2016. Experimental study on the inhibition effect of miR-106a inhibitor on tumor growth of ovarian cancer xenografts mice. Asian Pac. J. Trop. Med. 9, 698–701. https://doi.org/10.1016/j.apjtm.2016.05.008.

Chang, H., Zhou, X., Wang, Z.N., Song, Y.X., Zhao, F., Gao, P., et al., 2012. Increased expression of miR-148b in ovarian carcinoma and its clinical significance. Mol. Med. Rep. 5, 1277–1280. https://doi.org/10.3892/mmr.2012.794.

Chen, L.L., 2016. The biogenesis and emerging roles of circular RNAs. Nat. Rev. Mol. Cell Biol. 17, 205. https://doi.org/10.1038/nrm.2015.32.

Chen, L., Zhang, S., Wu, J., Cui, J., Zhong, L., Zeng, L., et al., 2017. circRNA_100290 plays a role in oral cancer by functioning as a sponge of the miR-29 family. Oncogene 36, 4551–4561. https://doi.org/10.1038/onc.2017.89.

Du WW, Zhang C., Yang, W., Yong, T., Awan, F.M., Yang, B.B., 2017a. Identifying and characterizing circRNA-protein interaction. Theranostics 7, 4183–4191. https://doi.org/10.7150/thno.21299.

Du WW, Yang W., Chen, Y., Wu, Z.K., Foster, F.S., Yang, Z., et al., 2017b. Foxo3 circular RNA promotes cardiac senescence by modulating multiple factors associated with stress and senescence responses. Eur. Heart J. 38, 1402. https://doi.org/10.1093/eurheartj/ehw001.

Han, B., Chao, J., Yao, H., 2018. Circular RNA and its mechanisms in disease: from the bench to the clinic. Pharmacol. Ther. https://doi.org/10.1016/j.pharmthera.2018.01.010. S0163-7258:30017-2.

Hansen, T.B., Jensen, T.I., Clausen, B.H., Bramsen, J.B., Finsen, B., Damgaard, C.K., et al., 2013. Natural RNA circles function as efficient microRNA sponges. Nature 495, 384–388. https://doi.org/10.1038/nature11993.

Jeck, W.R., Sharpless, N.E., 2014. Detecting and characterizing circular RNAs. Nat. Biotechnol. 32, 453–461. https://doi.org/10.1038/nbt.2890.

Li, Y., Zheng, F., Xiao, X., Xie, F., Tao, D., Huang, C., et al., 2017. CircHIPK3 sponges miR-558 to suppress heparanase expression in bladder cancer cells. EMBO Rep. 18, 1646. https://doi.org/10.15252/embr.201643581.

Long, M.J., Wu, F.X., Li, P., Liu, M., Li, X., Tang, H., 2012. MicroRNA-10a targets CHL1 and promotes cell growth, migration and invasion in human cervical cancer cells. Cancer Lett. 324, 186–196. https://doi.org/10.1016/j.canlet.2012.05.022.

Memczak, S., Jens, M., Elefsinioti, A., Torti, F., Krueger, J., Rybak, A., et al., 2013. Circular RNAs are a large class of animal RNAs with regulatory potency. Nature 495 (7441), 333–338. https://doi.org/10.1038/nature11928.

Salmena, L., Poliseno, L., Tay, Y., Kats, L., Pandolfi, P.P., 2011. ceRNA hypothesis: The Rosetta Stone of a hidden RNA language? Cell 146, 353–358. https://doi.org/10.1016/j.cell.2011.07.014.

Shan, K., Liu, C., Liu, B.H., Chen, X., Dong, R., Liu, X., et al., 2017. Circular non-coding RNA HIPK3 mediates retinal vascular dysfunction in diabetes mellitus. Circulation 136 (17), 1629. https://doi.org/10.1161/CIRCULATIONAHA.117.029004.

Siegel, Rebecca L., Miller, K.D., Jemal, A., 2018. Cancer statistics. CA Cancer J. Clin. 68, 7–30. https://doi.org/10.3322/caac.21442.

Vaughan, S., Coward, J.I., Bast Jr, R.C., Berchuck, A., Berek, J.S., Brenton, J.D., et al., 2011. Rethinking ovarian cancer: recommendations for improving outcomes. Nat. Rev. Cancer 11, 719–725. https://doi.org/10.1038/nrc3144.

Wang, K., Long, B., Liu, F., Wang, J.X., Liu, C.Y., Zhao, B., et al., 2016. A circular RNA protects the heart from pathological hypertrophy and heart failure by targeting miR-223. Eur. Heart J. 37, 2602. https://doi.org/10.1093/eurheartj/ehv713.

Wang, Y., Mo, Y., Gong, Z., Xiang, Y., Mo, Y., Zhang, S., et al., 2017. Circular RNAs in human cancer. Mol. Cancer 16, 25. https://doi.org/10.1186/s12943-017-0598-7.

Weiss, F.U., Marques, I.J., Woltering, J.M., Vlecken, D.H., Aghdassi, A., Partecke, L.I., et al., 2009. Retinoic acid receptor antagonists inhibit miR-10a expression and block metastatic behavior of pancreatic cancer. Gastroenterology 137, 2136. https://doi.org/10.1053/j.gastro.2009.08.065.

Xu, P., Zhang, X., Miao, C., Fu, Z., Li, Z., Zhang, G., et al., 2013. Promotion of melanoma cell invasion and tumor metastasis by microcystin-LR via phosphatidylinositol 3-kinase/AKT pathway. Environ. Sci. Technol. 47 (15), 8801–8808. https://doi.org/10.1021/es4007228.

Yang, Q., Du WW, Wu N., Yang, W., Awan, F.M., Fang, L., et al., 2017. A circular RNA promotes tumorigenesis by inducing c-myc nuclear translocation. Cell Death Differ. 24, 1609. https://doi.org/10.1038/cdd.2017.86.

You, X., Vlatkovic, I., Babic, A., Will, T., Epstein, I., Tushev, G., et al., 2015. Neural circular RNAs are derived from synaptic genes and regulated by development and plasticity. Nat. Neurosci. 18, 603–610. https://doi.org/10.1038/nn.3975.

Zeng, K., Chen, X., Xu, M., Liu, X., Hu, X., Xu, T., et al., 2018. CircHIPK3 promotes colorectal cancer growth and metastasis by sponging miR-7. Cell Death Dis. 9 (417). https://doi.org/10.1038/s41419-018-0454-8.

Zheng, Q., Bao, C., Guo, W., Li, S., Chen, J., Chen, B., et al., 2016. Circular RNA profiling reveals an abundant circHIPK3 that regulates cell growth by sponging multiple miRNAs. Nat. Commun. 7 (11215). https://doi.org/10.1038/ncomms11215.

Zhong, Z., Huang, M., Lv, M., He, Y., Duan, C., Zhang, L., et al., 2017. Circular RNA MYLK as a competing endogenous RNA promotes bladder cancer progression through modulating VEGFA/VEGFR2 signaling pathway. Cancer. Lett. 403. https://doi.org/10.1016/j.canlet.2017.06.027.